Magnesium Technology 2011
Edited by: Wim H. Sillekens, Sean R. Agnew, Neale R. Neelameggham, and Suveen N. Mathaudhu
TMS (The Minerals, Metals & Materials Society), 2011

DEVELOPMENT AND CHARACTERIZATION OF NEW AZ41 AND AZ51 MAGNESIUM ALLOYS

Md Ershadul Alam[1], Samson Han[2], Abdelmagid Salem Hamouda[1], Quy Bau Nguyen[2] and Manoj Gupta[2]
[1] Department of Mechanical and Industrial Engineering, College of Engineering, Qatar University, Doha, Qatar 2713
[2] Department of Mechanical Engineering, National University of Singapore, 9 Engineering Drive 1, Singapore 117576

Keywords: Magnesium alloy, AZ31, AZ41, AZ51, Mechanical properties.

Abstract

In the present study, new AZ41 and AZ51 magnesium alloys were successfully synthesized by adding 1 wt. % and 2 wt. % aluminum into AZ31B matrix, respectively, using an innovative disintegrated melt deposition technique followed by hot extrusion. Microstructural characterization studies revealed equiaxed grain morphology, reasonably uniform distribution of intermetallics in the matrix and minimal porosity. Physical properties characterization revealed that addition of Al reduced the coefficient of thermal expansion (CTE) of monolithic AZ31B. The presence of higher percentage of aluminum also assisted in improving overall mechanical properties including microhardness, modulus of elasticity, 0.2% yield strength, ultimate tensile strength, and work of fracture of AZ31. The results suggest that these newly developed AZ magnesium alloys have significant potential in diverse engineering applications when compared to AZ31 alloy.

Introduction

Increasing demand for the reduction of fuel consumption and environmental problems has led to intensive research effort into the design and development of light structural materials [1, 2]. Consequently, magnesium alloys are attracting much attention as light weight materials. Magnesium, with a density of 1.74 g/cm^3, is the lightest engineering metal available in the earth which is about two-thirds of the density of aluminum (2.70 g/cm^3) and one-quarter of that of iron (7.87 g/cm^3) [3]. Hence, its use is gaining significance in certain key engineering applications, particularly in automobile, aviation, electronics and consumer industries where weight is one of the most important criteria in the choice of materials [1,2, 4-7]. Besides low density, magnesium based materials exhibit good specific mechanical properties, machinability, castability, weldability, thermal stability, damping and resistance to electromagnetic radiation [8]. However, as magnesium has low ductility, modulus of elasticity and limited strength and creep resistance at elevated temperature, it cannot be extensively applied in structural applications [4-9]. Therefore, magnesium is rarely used in its pure form. Instead, it is usually alloyed with other elements like aluminum, zinc, silver and zirconium to improve its properties like corrosion resistance and ductility [1, 8-11]. Among these alloying constituents, the addition of aluminum seems to have the most favorable effect on magnesium, exhibiting much greater strength and hardness. Even though there has been extensive research and characterization on magnesium-aluminum alloys, it has mainly focused on specific compositions, like AZ31 (3 wt.% Al, 1 wt.% Zn, remaining Mg), AZ61 (6 wt.% Al, 1 wt.% Zn, remaining Mg) and AZ91 (9 wt.% Al, 1 wt.% Zn, remaining Mg) [8, 9-12]. Results of open literature search shows that only a few research groups have worked on developing and characterizing AZ41 sheets, mainly by twin-roll-cast technique [13-16], while Kim *et al.*[17] synthesized and characterized AZ51 alloys that contained pure Sn up to 9 wt%. No results are reported in which investigators have synthesized AZ41 and AZ51 alloys by incorporating 1 and 2 wt. % elemental Al, respectively, by superheating with AZ31B using DMD technique. Accordingly, in the present study, new AZ41 and AZ51 magnesium based alloys were synthesized and characterized their properties.

Characterization studies were carried out on these formulations to investigate their physical, microstructural and mechanical properties. These include density and porosity measurements, the coefficient of thermal expansion, grain morphology, x-ray diffraction analysis, optical and scanning electron microscopy, microhardness, tensile tests and fractography studies.

Experimental Procedures

Materials

In the present study, AZ31B magnesium alloy ingots (2.94% Al, 0.87% Zn, 0.57% Mn, 0.0027% Fe, 0.0112% Si, 0.0008% Cu, 0.0005% Ni and balance Mg, supplied by Tokyo Magnesium Company, Japan) were used as a matrix material and cut into small pieces so that they can be placed into the graphite crucible easily. The aluminum lumps of 99.5% purity (supplied by Alfa Aesar, USA) were also used for developing new AZ41 and AZ51 alloys.

Primary Processing

Synthesis of AZ31, AZ41 and AZ51 magnesium based alloys was carried out using disintegrated melt deposition (DMD) technique. Synthesis of the AZ41 and AZ51 alloys involved heating the AZ31B magnesium alloy pieces with the addition of 1 and 2 wt.% Al, respectively, to 750 ^{0}C in an inert Ar gas atmosphere in a graphite crucible using a resistance heating furnace. The crucible was equipped with an arrangement for bottom pouring. Upon reaching the superheat temperature, the molten slurry was stirred for 5 min at 450 rev./min using a twin blade (pitch 45^0) mild steel impeller to facilitate the incorporation and uniform distribution of reinforcement particulates in the metallic matrix. The impeller was coated with Zirtex 25 (86% ZrO_2, 8.8% Y_2O_3, 3.6% SiO_2, 1.2% K_2O and Na_2O, and 0.3% trace inorganic) to avoid iron contamination of the molten metal. The melt was then released through a 10-mm diameter orifice at the base of the crucible. The melt material was disintegrated by two jets of argon gas orientated normal to the melt stream. The argon gas flow rate was maintained at 25 L /min. The disintegrated alloy melt slurry was subsequently deposited onto a metallic substrate. Preform of 40-mm diameter was obtained following the deposition stage. The synthesis of monolithic AZ31 magnesium alloy was carried out using steps similar to those employed for the AZ41 and AZ51 alloys except that no Al lumps were added.

Secondary Processing

Pre-Extrusion: The 40 mm diameter ingots were machined down using a lathe machine to a diameter of 36 mm and cut into billets with heights of approximately 45 mm. They were then lathed in the direction perpendicular to the length of the ingot to ensure both ends are flat and perpendicular to the surface. The billets were then sprayed with colloidal graphite for lubrication purposes.

Extrusion: The billets were first soaked at 400 ^{0}C for 60 minutes in a constant temperature furnace before extrusion. Extrusion was performed on a 150 tonne hydraulic press using an extrusion ratio of 20.25:1, producing rods of 8 mm diameter.

Post-Extrusion: After extrusion, the extruded rods were machined to produce tensile specimens. Sections of approximately 10 to 15 mm in height were also cut by a low speed diamond blade and the surface graphite was then cleaned-off to use for various characterization studies.

Density and Porosity Measurements

Density (ρ) measurements were performed in accordance with Archimedes' principle on three randomly selected polished samples of AZ31, AZ41 and AZ51 alloys taken from the extruded rods. Distilled water was used as the immersion fluid. The samples were weighed using an A&D ER-182A electronic balance; with an accuracy of ±0.0001 g. Theoretical densities of materials were calculated assuming they are fully-dense. Rule-of-Mixture was used in all calculations. The porosity was calculated by using the theoretical and experimental densities.

Microstructural Characterization

Microstructural characterization studies were conducted on metallographically polished extruded samples to investigate morphological characteristics of grains, reinforcement distribution and interfacial integrity between the matrix and reinforcement. The etching solution (5 ml acetic acid, 6 g picric acid, 10 ml water and 100 ml ethanol) was applied for approximately 20 seconds using a swabbing technique and then washed under running water to reveal the grain boundaries [8, 18]. The sample was then analyzed using the Olympus BH2-UMA metallographic optical microscope equipped with Olympus DP-10 microscope digital camera. The grain boundaries were then traced out from the micrographs with the aid of the Adobe Photoshop program. Image analysis using the Scion system was carried out to determine the grain size of the materials.

The presence and distribution of the intermetallic phase was investigated using the JEOL JSM-5600LV Scanning Electron Microscope (SEM). Polished specimens were observed at 1000x magnification to reveal the intermetallic phase. Images were captured at an accelerating voltage of 15 kV and spot size of 20.

X-Ray Diffraction Studies

X-ray diffraction analysis was conducted using the automated Shimadzu LAB-X XRD-6000 x-ray diffractometer. Flat, ground and ultrasonically cleaned specimens of approximately 5 mm in height were exposed to CuK_α radiation (λ = 1.54056 Å) with a scanning speed of 2 ^{0}/min. The scanning range was 30^0 to 80^0 for all samples. A plot of intensity against 2θ (θ represents Bragg angle) was obtained, illustrating peaks at different Bragg angles. The Bragg angles corresponding to different peaks were noted; and the values of interplanar spacing (d-spacing) obtained from the computerized output were compared with the standard values from the International Centre for Diffraction Data's Powder Diffraction File (PDF).

Coefficient of Thermal Expansion

The coefficients of thermal expansion (CTE) of all the compositions were determined by measuring the displacement of the samples as a function of temperature in the temperature range of 50 ^{0}C- 400 ^{0}C using an automated SETARAM 92-16/18 thermo-mechanical analyzer.

Mechanical Characteristics

The mechanical properties carried out on all samples were investigated by conducting tensile and microhardness tests. All experiments were carried out at room temperature.

Microhardness Test: The microhardness tests were conducted on flat and metallographically polished specimens. The test was conducted using a Shimadzu HMV automatic digital microhardness tester with a Vickers indenter (square-based pyramidal-shaped diamond indenter with face angle of 136 ^{0}). An indenting load of 25 gf and a dwell time of 15 seconds were used. Testing was performed in accordance with ASTM test standard E384-08. Indentations were performed on the matrix and measurements were recorded in Vickers Hardness (HV).

Tensile Testing: The tensile properties of each sample were determined in accordance with ASTM test standard E8M-08. Round tension test specimens of 5 mm in diameter were machined from the 8 mm extruded rod. An average of five tensile specimens could be obtained from a single rod, and a minimum of four tensile tests were conducted for each sample. Tests were performed on the 810 Material Test System (MTS) with an extensometer of 25 mm gauge length and a crosshead speed of 0.254 mm/min was used. The raw stress-strain data recorded was extracted to be analyzed. Broken test specimens were labeled individually, carefully handled and packed into individual plastic bags to prevent damage of the fractured surface. A Microsoft Excel program was written to analyze the raw data extracted. Then, the modulus of elasticity (E), 0.2% offset yield strength (0.2% YS), ultimate tensile strength (UTS) and failure strain was computed via a series of Microsoft Excel functions. The work of fracture was also computed in the program by the use of the trapezium rule.

Fracture Behavior: The fracture surfaces of the broken tensile samples were analyzed to investigate the failure mechanisms that occurred during the tensile tests. Fractography studies were performed on the JEOL JSM-5600LV Scanning Electron Microscope. Images were captured at an accelerating voltage of 15 kV and a working distance of about 25 mm. Macromechanism of these fracture surfaces were also investigated.

Results

Macrostructure

The result of macrostructural characterization conducted on the as deposited monolithic AZ31B and alloyed materials did not reveal

any presence of macropores, shrinkage, cracks or any other defects. Following extrusion, there was also no evidence of any macrostructural defects.

Density and Porosity Measurements

The results of the density measurements are shown in Table I. Results show that near dense monolithic AZ31B and alloyed AZ41 and AZ51 can be developed using the fabrication methodology adopted in the present study.

Table I. Results of Density and Porosity Measurements

Materials	Al (wt. %)	Density (g/cm^3)		Porosity (%)
		Theo.	Expt.	
AZ31	-	1.776	1.775	0.05
AZ41	1.0	1.786	1.785	0.05
AZ51	2.0	1.792	1.791	0.08

Microstructural Characteristics

Microstructural studies conducted on the extruded specimens showed near equiaxed grain morphology (see Table II and Figure 1). Average grain size of AZ31B samples decreased with the addition of Al. However, the variation of grain size among the samples, especially between the AZ41 and AZ51 alloys is statistically insignificant considering standard deviation.

Table II. Results of Grain Morphology

Materials	Grain Size (μm)	Aspect Ratio	Roundness[1]
AZ31	4.1 ± 1.8	1.5 ± 0.4	1.5 ± 0.4
AZ41	2.9 ± 1.3	1.6 ± 0.4	1.6 ± 0.6
AZ51	2.8 ± 1.3	1.7 ± 0.5	1.7 ± 0.7

1. Roundness is the shape of the grain expressed by the formula (perimeter)^2 / 4π (area)

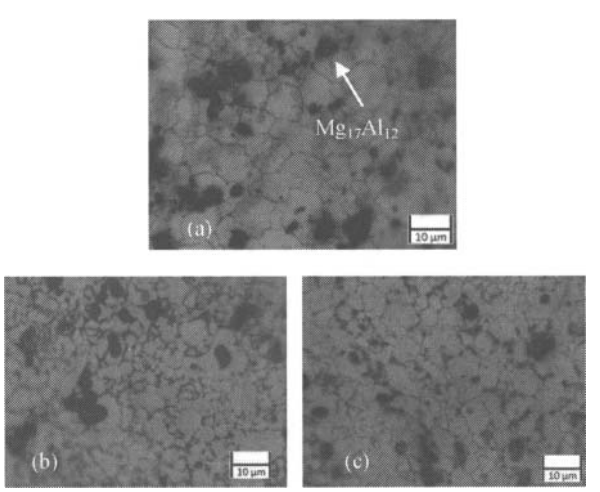

Figure 1. Representative optical micrographs showing the grain morphology (1000x) of: (a) AZ31B, (b) AZ41 and (c) AZ51 samples, respectively.

Microstructural characterization studies were also conducted on the extruded and polished samples to observe the shape and distribution of intermetallic phases in the matrix (see Figure 2).

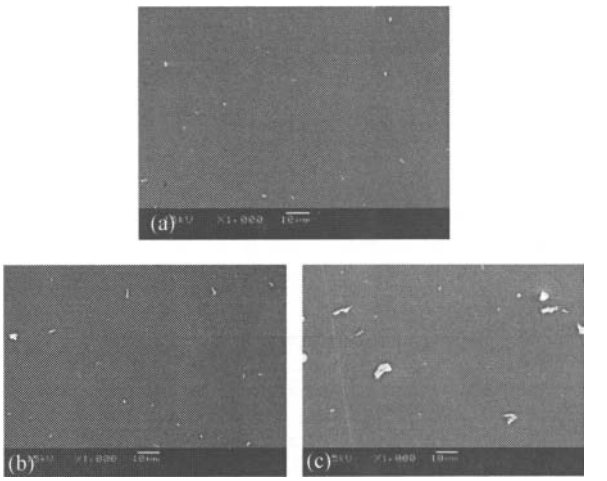

Figure 2. Representative SEM micrographs showing the shape and distribution of second phase in the case of: (a) AZ31B, (b) AZ41 and (c) AZ51 samples, respectively.

X-Ray Diffraction

X-ray diffraction (XRD) was carried out on all extruded samples (see Table III). The obtained lattice spacing's (d-spacing) and two-theta (2θ) value were compared with the standard values for magnesium and the Mg-Al intermetallic phases. Results showed the presence of intermetallic $Al_{12}Mg_{17}$ phase in the α-Mg phase.

Table III. Results of XRD and CTE Analysis

Materials	Mg	$Mg_{17}Al_{12}$	CTE (μm/mK)
AZ31	11[3]	1[1]	28.8
AZ41	11[3]	1[1]	27.1
AZ51	11[3]	2[1]	27.0

Coefficient of Thermal Expansion

Table III shows the results of coefficient of thermal expansion measurements obtained from AZ31, AZ41 and AZ51 samples. The results revealed a reduction in CTE of the AZ31B matrix with the addition of Al.

Mechanical Characteristics

Microhardness Test: Vickers microhardness tests were conducted on all extruded and polished samples (see Table IV). Results revealed that the addition of Al increased the microhardness value of AZ31 matrix. Around 29% microhardness value was increased when 2 wt. % aluminum was added into AZ31B to develop AZ51 magnesium alloy. Moreover, AZ51 magnesium alloy exhibited

37% higher hardness when compared to commercial AZ61A alloy (see Table IV) [3].

Table IV. Results of Room Temperature Microhardness and Modulus of Elasticity Tests

Materials	Microhardness (HV)	Modulus of Elasticity (GPa)
AZ31	66±2	34 ± 4
AZ41	77±3	65 ± 4
AZ51	85±3	69 ± 1
AZ61A [3]	62	45

Tensile Test: Results of ambient temperature tensile test on round tensile specimens revealed that the addition of Al in AZ31 magnesium increased the modulus of elasticity, 0.2% yield strength (YS) and ultimate tensile strength (UTS) (see Tables IV and V). In the case of AZ41 and AZ51 magnesium alloys, modulus of elasticity was increased around 91% and 103%, respectively, when compared to monolithic AZ31B. Results also showed that the AZ51 alloy exhibited 53% higher modulus of elasticity when compared to the commercial AZ61A magnesium alloy (see Table IV) [3]. However, failure strain (FS) dropped with the addition of Al while work of fracture (WoF) between AZ31 and AZ51 remained statistically unchanged.

Table V. Results of Room Temperature Tensile Properties

Matsrials	0.2 % YS (MPa)	UTS (MPa)	FS (%)	WoF (MJ/m^3)
AZ31	180 ± 3	273 ± 6	10.6 ± 1.3	27.9 ± 3.9
AZ41	218 ± 5	287 ± 6	8.2 ± 0.3	23.0 ± 1.4
AZ51	222 ± 4	302 ± 4	8.7 ± 0.4	27.3 ± 1.2
AZ61A [3]	228	310	16	-

Fracture Behavior: Macroscopic fracture characteristics of the broken tensile samples revealed that all samples exhibited shear-type ductile fracture mode. Microscopic features of fracture surface were also conducted on the tensile fractured surface using SEM and dimple-like features were observed in all the cases.

Discussion

Macrostructure

Synthesis of AZ31, AZ41 and AZ51 alloys were successfully accomplished by using DMD technique followed by hot extrusion. Observations made during DMD processing revealed: (a) minimal oxidation of melts, (b) undetectable reaction between graphite crucible and melts (AZ31, AZ41 and AZ51) and (c) absence of blowholes and macropores. The results suggest the appropriateness of processing parameters and methodology used in the present study. These observations are also consistent with the previous findings made on DMD processed magnesium based materials [1, 8, 10].

Density and Porosity Measurements

The experimental density obtained by the Archimedes' principle exhibited that the density of newly developed magnesium based materials increased negligibly with the addition of elemental Al into AZ31 matrix (see Table I). This can be attributed to the relatively higher dense Al (2.70 g/cm^3) addition into AZ31 matrix (1.78 g/cm^3) [3, 8]. Obtained results also revealed that the experimental values were relatively close to the theoretical values. This indicated that the experimental method used was accurate, and the experimental density of the fabricated materials could be calculated.

Porosity of the materials was calculated using the theoretical and the experimental densities obtained from each sample. The highest porosity obtained among the samples was 0.08% (see Table I), hence indicating that near dense materials was obtained and that the alloying constituent was successfully incorporated into the matrix. Therefore, as demonstrated by prior studies, the fabrication route of DMD followed by hot extrusion is capable of producing new AZ41 and AZ51 alloys with minimal porosity [8].

Microstructural Characteristics

The results of microstructural characterization revealed the presence of nearly equiaxed grains (see Table II and Figure 1) in AZ31, AZ41 and AZ51 samples. β-$Mg_{17}Al_{12}$ phase predominantly located at grain boundaries was observed in all samples (see Figure 1). Addition of elemental Al into AZ31 matrix decreased the average grain boundaries. This can be attributed to the pinning of grain boundaries by the increasing amount of second phases resulting in limited grain growth.

Optical and SEM micrographs of the etched samples revealed the presence and good distribution of the equilibrium intermetallic phase $Mg_{17}Al_{12}$ (see Figures 1 and 2). This could be attributed to the use of a layered arrangement for the raw materials during the solidification process and effective stirring parameters. The successful disintegration of the melt and the inert atmosphere caused by the argon gas jets were also the contributing factors. In the AZ41 system, the intermetallic particles appeared to have sharp edges. At these boundaries, the local stress concentration will be higher than that of the AZ31 system, which has blunt edges (see Figure 2). In contrast, these intermetallic phases became blunt with the addition of 2 wt% of Al into AZ31 matrix, thereby lowering the local stress concentration (see Figure 2).

X-Ray Diffraction

X-Ray diffraction results confirmed the presence of the intermetallic phase $Mg_{17}Al_{12}$ in all of the compositions (see Table III). For AZ51 samples, increased number of intermetallic peaks can be observed indicating higher amount of second phase were formed when compared to the AZ31 and AZ41 systems.

Coefficient of Thermal Expansion

The results of CTE measurement showed that the addition of Al alloying constituent into AZ31B matrix decreases the average CTE values of the materials (see Table III). The results suggested an appropriate integration of AZ31B alloy with elemental Al leading to low CTE values. Moreover, the lower CTE values of Al

(23.6 μm/mK) than Mg (25.2 μm/mK) also helped to lower the average CTE value of the newly developed compositions [3].

Mechanical Characteristics

Microhardness Test: The experimental results of microhardness measurement are shown in Table IV. AZ31 magnesium exhibited the lowest average hardness value and the average microhardness increased by about 17 % and 29% with the addition of 1 wt. % and 2 wt. % Al, respectively, into AZ31B. This can be attributed to the lower average grain size of these new compositions when compared to AZ31 which is associated with larger grain boundary area leading to higher hardness [19, 20]. The increase in hardness can be attributed to: (i) the presence of relatively harder elemental Al in the matrix, (ii) the reasonably uniform distribution of harder $Mg_{17}Al_{12}$ intermetallic in the matrix and (iii) higher constraint to the localized matrix deformation during indentation due to the higher presence of the intermetallic [21, 22].

Tensile Test: The elastic modulus measurement revealed that the addition of elemental Al into AZ31B system helped to increase the modulus of elasticity (see Table IV). The elastic modulus or stiffness of AZ51 samples was up to 103% higher than that of AZ31B samples. Increase in modulus was expected due to: (a) the addition of higher modulus of Al (69 GPa) into Mg (38 GPa) based compositions and (b) uniform distribution of second phase with good interfacial integrity [23, 24].

Room temperature tensile test results revealed that the addition of elemental Al increased the strength of monolithic AZ31 magnesium (~ 23% increment of 0.2% YS and ~11% increment of UTS in case of 2 wt. % Al addition) (see Table V and Figure 3). This can be attributed to the lower average grain size of AZ41 and AZ51 samples when compared to AZ31 samples (see Table II and Figure 1). Presence of additional Al modified the microstructural features, hence increasing strength. This follows a trend as the strength level of AZ61 and AZ91 is higher than that of AZ31 [3]. Failure strain decreased with Al addition into AZ31 magnesium. This can be attributed to the formation and presence of sharp edge intermetallic particles which might act as a stress concentration sites (see Figure 2). Work of fracture also dropped for AZ41 magnesium when compared to AZ31 magnesium. This can be attributed to the lower area under the stress-strain curve as the ductility of AZ41 is lower than AZ31. However, WoF of AZ51 samples remain unchanged when compared to AZ31B and increased when compared to AZ41 samples.

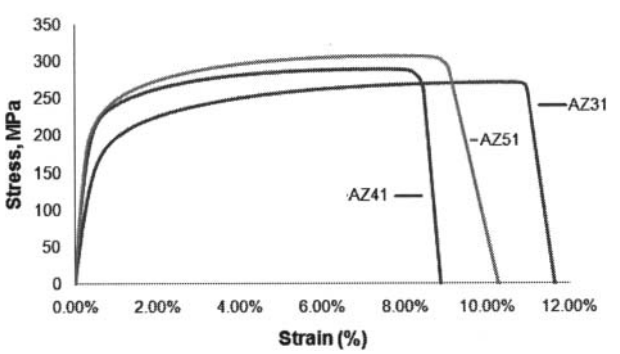

Figure 3. Engineering stress-strain diagram of AZ31, AZ41 and AZ51 samples.

Fracture Behavior: Macroscopic observations performed on the broken tensile samples revealed shear type fracture characteristics. Microscopic observations showed that dimple like features were predominately present in all compositions, indicating high plastic deformation (see Figure 4). However, more presence of microcracks were observed for new systems, hence are responsible for the decrease in failure strain of these composites.

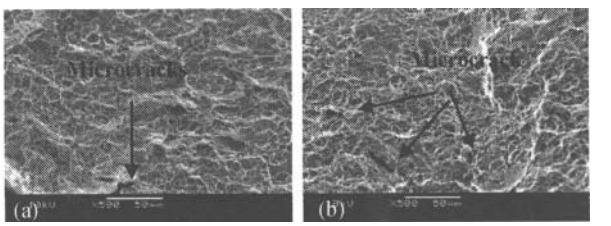

Figure 4. Representative SEM fractographs showing the microcracks and dimple like features for: (a) AZ31 and (b) AZ51 samples, respectively.

Conclusions

The following conclusions can be made from the present study:

1. Monolithic AZ31, AZ41 and AZ51 alloys can be successfully synthesized by using the disintegrated melt deposition technique followed by hot extrusion with minimal porosity.
2. The microstructure of all the AZ systems developed in this study consists of the magnesium phase and the intermetallic phase, $Mg_{17}Al_{12}$.
3. The coefficient of thermal expansion of AZ31 magnesium decreases with the addition of elemental aluminum.
4. Microhardness and modulus of elasticity values increase with the elemental Al addition as an alloying element to AZ31 magnesium.
5. A good combination of tensile properties (in terms of 0.2% YS, UTS and WoF) was observed for AZ41 and AZ51 samples when compared to AZ31B samples. These newly developed AZ magnesium based materials have significant potential in diverse engineering applications when compared to AZ31 alloy.

Acknowledgments

The authors gratefully acknowledge the support received for this research work ref: NPRP 08-424-2-171 from the Qatar National Research Fund (QNRF), Qatar.

References

[1] S. F. Hassan and M. Gupta, "Development of Nano-Y_2O_3 Containing Magnesium Nanocomposites Using Solidification Processing", Journal of Alloys and Compounds, 429 (1-2) (2007) 176-183.

[2] R. Fink, in: K. U. Kainer (Ed.), "Die-Casting Magnesium, Magnesium Alloys and Technologies", (Wiley-VCH Verlag GmbH and Co., Germany, 2003) 23-44.

[3] J. R. Davis, "Properties and Selection: Nonferrous Alloys and Special-Purpose Materials", Formerly Tenth Edition, (ASM Handbook, Volume 2, ASM, Metal Park, Ohio, 1993) 480-515, 1099-1100, 1118-1128,1199, 1132-1135.

[4] B. L. Mordike and K. U. Kainer, "Magnesium Alloys and Their Applications", (Werkstoff-Informationsgesellschaft, Frankfurt, Germany, 1998).

[5] B. L. Mordike and T. Ebert, "Magnesium: Properties-Applications-Potentials", Mater. Sci. Eng. A, 302 (2001) 137-45.

[6] D. J. Lloyd, "Particle Reinforced Aluminium and Magnesium Matrix Composites", Int. Mater. Rev., 39 (1994) 1-23.

[7] F. Moll and K. U. Kainer, "Magnesium Alloys and Technology", Kainer, K. U. (Ed), (Weinheim: Wiley-VCH, Germany, 2002) 197-217.

[8] Q. B. Nguyen and M. Gupta, "Increasing Significantly the Failure Strain and Work of Fracture of Solidification Processed AZ31B Using Nano-Al_2O_3 Particulates", J. Alloys Compd., 459 (2008) 244-250.

[9] W. Westengen, "Magnesium: Alloying", Encyclopedia of Materials: Science and Technology, (2008) 4739-4743.

[10] S. F. Hassan, K. F. Ho and M. Gupta, "Increasing Elastic Modulus, Strength and CTE of AZ91 by Reinforcing Pure Magnesium with Elemental Copper", Mater. Letters, 58 (2004) 2143-2146.

[11] K. Hirai, H. Somekawa, Y. Takigawa and K. Higashi, "Effects of Ca and Sr Addition on Mechanical Properties of a Cast AZ91 Magnesium Alloys at Room and Elevated Temperature", Mater. Sci. Eng. A, 403 (2005) 276-280.

[12] Presentations from Elektron 21 product launch CD provided by Magnesium Elektron, UK http://www.magnesium-elektron.com/site-map.asp (accessed on 26 September' 2010).

[13] X. Gong, H. Li, S. B. Kang, J. H. Cho and S. Li, "Microstructure and Mechanical Properties of Twin-Roll-Cast Mg-4.5Al-1.0Zn Sheets Produced by Differential Speed Rolling", Materials and Design, 31 (2010) 1581-1587.

[14] H. M. Chen, H. S. Yu, S. B. Kang and G. H. Min, "Optimization of Annealing Treatment Parameters in a Twin-Roll-Cast and Warm Rolled Mg-4.5Al-1.0Zn Alloy", Advanced Materials Research, 79-82 (2009) 2139-2142.

[15] S. Wang, M. Wang, R. Ma, Y. Wang and Y. Wang, Microstructure and Hot Compression Behavior of Twin-Roll-Casting AZ41M Magnesium Alloy", Rear Metals, 29 (2010) 396-400.

[16] K. Matsuzaki, K. Hatsukano, Y. Torisaka, K. Hanada, T. Shimizu and M. Kato, "Microstructure and Mechanical Properties of Mg Alloy Sheets Produced by Twin-Roll-Caster", Materials Science Forum, 539-543 (2007) 1747-1752.

[17] B. H. Kim, J. J. Jeon, K. C. Park, B. G. Park, Y. H. Park and I. M. Park, "Microstructural Characterization and Mechanical Properties of Mg-xSn-5Al-1Zn Alloys", International Journal of Cast Metals Research, 21 (2008) 186-192.

[18] A. Jager, P. Lukac, V. Gartnerova, J. Haloda, and M. Dopita, "Influence of Annealing on the Microstructure of Commercial Mg Alloy AZ31 after Mechanical Forming", Mater. Sci. Eng. A, 432 (2006) 20-25.

[19] G. E. Dieter, "Mechanical Metallurgy", (2nd Edition, McGraw-Hill, Inc., USA, 1976) 191-193.

[20] M. E. Alam and M. Gupta, "Tensile Behavior of Tin Sintered Using Microwave and Radiant Heating", International Conference on Mechanical Engineering (ICME' 07), December 29-31, 2007, Dhaka, Bangladesh.

[21] M. Paramsothy, N. Srikanth and M. Gupta, "Solidification Processed Mg/Al Bimetal Macrocomposite: Microstructure and Mechanical Properties", J. Alloys Compd., 461 (2008) 200-208.

[22] M. E. Alam, S. M. L. Nai and M. Gupta, "Development of High Strength Sn-Cu Solder Using Copper Particles at Nanolength Scale", Journal of Alloys and Compounds, 476 (2009) 199-206.

[23] M. Paramsothy, S. F. Hassan, N. Srikanth and M Gupta, "Enhancing the Performance of Magnesium Alloy AZ31 by Integration with Millimeter Length Scale Aluminium Based Cores", J. Comp. Mater., 44 (9) (2010) 1099-1117.

[24] S. F. Hassan and M. Gupta, "Development of High Strength Magnesium Based Composites using Elemental Nickel Particulates as Reinforcement", Journal of Mateials science, 37 (2002) 2467-2474.